UNCLASSIFIED

NACA

RESEARCH MEMORANDUM

for the

Bureau of Aeronautics, Department of the Navy

PRELIMINARY RESULTS OBTAINED FROM FLIGHT TEST OF A

ROCKET MODEL HAVING THE TAIL ONLY OF THE

GRUMMAN XF10F AIRPLANE CONFIGURATION

TED NO. NACA DE 354

By William N. Gardner and James L. Edmondson

Langley Aeronautical Laboratory
Langley Field, Va.

NATIONAL ADVISORY COMMITTEE

FOR AERONAUTICS

WASHINGTON

NATIONAL ADVISORY COMMITTEE FOR AERONAUTICS

RESEARCH MEMORANDUM

for the

Bureau of Aeronautics, Department of the Navy

PRELIMINARY RESULTS OBTAINED FROM FLIGHT TEST OF A

ROCKET MODEL HAVING THE TAIL ONLY OF THE

GRUMMAN XF10F AIRPLANE CONFIGURATION

TED NO. NACA DE 354

By William N. Gardner and James L. Edmondson

SUMMARY

A flight test was made to determine the servoplane effectiveness and stability characteristics of the free-floating horizontal stabilizer to be used on the XF10F airplane. The results of this test indicate that servoplane effectiveness is practically constant through the speed range up to a Mach number of 1.15, and the stabilizer static stability is satisfactory. A loss of damping occurs over a narrow Mach number range near $M = 1.0$, resulting in dynamic instability of the stabilizer in this narrow range. Above $M = 1.0$ there is a gradual positive trim change of the stabilizer.

INTRODUCTION

At the request of the Bureau of Aeronautics, Department of the Navy, the Langley Pilotless Aircraft Research Division is investigating the aerodynamic characteristics of the Grumman XF10F airplane through the use of rocket-propelled scale models. This paper presents the results obtained from the flight test of a wingless rocket-powered vehicle having a $\frac{1}{7}$- scale complete tail of the Grumman XF10F airplane configuration. The purpose of this test was to determine the static and dynamic stability characteristics of the free-floating horizontal tail, and to determine the effectiveness of the canard-type servoplane.

SYMBOLS

q   dynamic pressure, pounds per square foot

S   stabilizer area, square feet

V   velocity, feet per second

M   Mach number

$\bar{c}$ stabilizer mean aerodynamic chord, feet

$T_{1/2}$ time to damp to half-amplitude, seconds

P   period, seconds

α angle of attack, degrees

δ stabilizer deflection relative to body center line, degrees

δ_c servoplane deflection relative to stabilizer, degrees

C_{m_δ} rate of change of stabilizer pitching moment about pivot point

        with stabilizer deflection, $\dfrac{\partial C_m}{\partial \delta}$

$C_{m_{\dot{\delta}}}$ rate of change of stabilizer pitching moment about pivot point

        with rate of change of stabilizer deflection, $\dfrac{\partial C_m}{\partial \dfrac{d\delta}{dt}}$

I_Y moment of inertia of stabilizer about pivot point, slug-feet
        square

INSTRUMENTATION AND TESTS

The model was equipped with instruments for measuring the following
quantities: longitudinal acceleration, normal acceleration, total head
pressure, static pressure, angle of attack, stabilizer deflection, and
servoplane deflection. These data were obtained by means of the NACA
telemetering system and additional data were obtained from CW Doppler
radar, tracking radar, and radiosonde. The method of conducting the

test was to pulse the servoplane in a square wave at an approximate
frequency of one cycle per second and observe the resulting transient
response of the model and horizontal tail. The servoplane was pulsed
over a deflection range of $1°$ to $-2°$, and the stabilizer was provided
with deflection stops at $2°$ and $-5°$. The moment of inertia of the com-
plete horizontal-tail assembly was measured to be 0.1432 slug-feet
square about the pivot point. All derivatives and coefficients herein
presented are based on the stabilizer area and mean aerodynamic chord.

Figure 1 is a photograph of the model booster combination mounted
on the launching platform. Figure 2 is a time history of Mach number,
velocity, and dynamic pressure. Booster separation occurred at 3 sec-
onds after firing and the sustainer igniter fired at 11 seconds; how-
ever, the sustainer motor failed to ignite until 30 seconds. The total
flight time was 48 seconds and continuous data were obtained throughout
the flight after 7 seconds. The Mach number range covered in the test
was from 0.6 to 1.2.

RESULTS AND DISCUSSION

Dynamic Stability

The dynamic stability of the horizontal tail is indicated by the
time required for an oscillation following a control pulse to damp to
half-amplitude $T_{1/2}$, and by the damping derivative $C_{m_{\dot{\delta}}} = \dfrac{\partial C_m}{\partial \frac{d\delta}{dt}}$. Time
to damp to half-amplitude was determined by fairing a damping envelope
about an oscillation, and $C_{m_{\dot{\delta}}}$ was determined from the following rela-
tionship: $C_{m_{\dot{\delta}}} = \dfrac{4 I_Y V \left(\log_e 0.5 \right)}{57.3 q S \bar{c}^2 T_{1/2}}$.

Figures 3 and 4 are plots of $T_{1/2}$ and $C_{m_{\dot{\delta}}}$, respectively, against
Mach number. These data show a practically constant damping coefficient
at subsonic speeds and an extremely rapid loss of damping at $M = 0.97$
with the tail being dynamically unstable over a narrow Mach number range.
Above $M = 0.99$, damping is regained, and from $M = 1.0$ to $M = 1.1$,
$C_{m_{\dot{\delta}}}$ has approximately the same value as at subsonic speeds. Very little
supersonic damping data were obtained from the flight because a trim
change resulted in the tail's being against the positive stop for a
large portion of the time above $M = 1$. This trim characteristic will
be discussed in a later paragraph. The data of figures 3 and 4 also show
that the tail-damping characteristics are different for the two servo-
plane positions. At this time, it is not possible to establish definitely

whether the damping varies with servoplane position or whether it varies with stabilizer deflection, since only two servoplane positions were tested and the stabilizer oscillated over a different range for the two servoplane positions. However, it would appear more likely that the damping varies with stabilizer deflection, since the difference in servoplane deflections is relatively small.

Figure 5(a) presents a typical plot of a subsonic oscillation and damping envelope with the mean line of the oscillation straightened. Figure 5(b) is a plot of the oscillation and damping envelope with straightened mean line which shows the loss of damping and dynamic instability which occurred over a very narrow Mach number range. In each case, the values of $\Delta\delta$ shown are relative to the mean line of the oscillation and are not actual stabilizer positions. The true mean line in all cases was oscillating over a comparatively large range at low frequencies corresponding to the angle-of-attack variation of the model.

Static Stability

The static stability of the horizontal tail is indicated by the period P of the oscillation following a control pulse, and the period of oscillation is a measure of the rate of change of pitching moment of the stabilizer about the pivot point with stabilizer deflection, $C_{m_\delta} = \dfrac{\partial C_m}{\partial \delta}$. In determining values of C_{m_δ}, the effect of damping was considered to be small and was neglected.

Figure 6 is a plot of the variation of the period of oscillation of the stabilizer with Mach number, and figure 7 is a plot of the variation of C_{m_δ} with Mach number. C_{m_δ} is fairly constant at subsonic speeds and at a Mach number of 0.94 starts a gradual increase up to $M = 1.1$. The value of C_{m_δ} at $M = 1.1$ is about 30 percent greater than at $M = 0.94$. This increase in static stability is primarily due to the rearward movement of the center of pressure on the stabilizer. Again, as in the case of damping, the values of C_{m_δ} are different for the two servoplane positions. Since the stabilizer oscillated over different deflection ranges for the two servoplane positions, it is believed that this difference in C_{m_δ} values is due to the difference in stabilizer deflection range and not to the difference in servoplane position. The mean line of an oscillation occurring after a servoplane pulse is variable, and therefore it is difficult to establish a consistent variation of period with stabilizer deflection. However, close examination of the data obtained reveals a trend which shows lower values of C_{m_δ} at negative stabilizer deflections than at positive deflections. It

should be pointed out that the period data presented represent an average period throughout one complete pulse and these values were used in computing values for C_{m_δ}.

Another indication of the static stability of the horizontal tail is the rate of change of stabilizer deflection with angle of attack of the complete model, $\partial\delta/\partial\alpha$. These data are an indication of the rate of change of stabilizer pitching moment about the pivot point with angle of attack, $C_{m_\alpha} = \dfrac{\partial C_m}{\partial\alpha}$. Figure 8 is a plot of $\partial\delta/\partial\alpha$ at $\alpha = 0$ against Mach number and shows that $\partial\delta/\partial\alpha$ decreases to a very low value at $M = 0.95$ and thereafter increases quite rapidly up to $M = 1.15$. At supersonic speeds, the value of $\partial\delta/\partial\alpha$ is approximately five times greater than at subsonic speeds. Again this large increase in static stability is primarily attributed to the rearward movement of the stabilizer center of pressure. For the sake of clarity, it should be pointed out that $\partial\delta/\partial\alpha$ data are only an indication of static stability of the stabilizer about the pivot point and are not an indication of the effectiveness of the stabilizer as a horizontal tail. These $\partial\delta/\partial\alpha$ data were obtained by measuring the slope of a plot of stabilizer trim position against α. The high values of $\partial\delta/\partial\alpha$ at supersonic speeds indicate that the contribution of the tail to airplane static stability and damping at supersonic speeds is much less than at subsonic speeds. Figure 9 is a plot of $\partial\delta/\partial\alpha$ against α at speeds below $M = 0.9$. These data show the variation of $\partial\delta/\partial\alpha$ over the angle of attack range and indicate that at high angles of attack corrresponding to negative stabilizer deflection the stabilizer approaches neutral stability insofar as C_{m_α} is concerned.

Servoplane Effectiveness

Servoplane effectiveness, as indicated by $\dfrac{\Delta\delta}{\Delta\delta_c}$, is presented in figure 10. These data were obtained by determining the difference in trim stabilizer deflection at zero angle of attack for the two servoplane positions. The significant factor shown by these data is that servoplane effectiveness is practically constant with Mach number up to $M = 1.15$.

Trim Characteristics

Figure 11 is a plot of trim stabilizer position against angle of attack. This curve represents typical subsonic and supersonic cases and is presented here as an illustration of the type of data obtained. The large amount of hysteresis present is due to a phase relationship existing between the two degrees of freedom, model pitching motion about the center of gravity, and stabilizer pitching motion about the pivot

point. This phase relationship is peculiar to this particular tail-alone model and is primarily a function of the relative mass and inertia characteristics of the model and stabilizer. The phase relationship which would occur on the full-scale airplane probably is entirely different from the present case and no direct comparison is possible. All of the associated data presented herein were obtained by fairing a mean line through the hysteresis loop. In comparing the subsonic and supersonic cases, two factors are outstanding. One which has already been discussed is the large increase in $\partial\delta/\partial\alpha$ at supersonic speeds. The other is the trim change at supersonic speeds.

Figure 12 is a plot against Mach number of the trim stabilizer deflection at zero angle of attack for each servoplane position. These data show a gradually increasing trim change in the positive direction, beginning at $M = 0.95$ and continuing on up to the positive deflection limit of the stabilizer as Mach number is increased. This trim-change characteristic resulted in the stabilizer's being against its positive stop, except at high positive angles of attack, during the supersonic portion of the flight, which limited the amount of supersonic data obtained. The trim change is relatively constant with changes in angle of attack and thus is not believed to be a function of angle of attack.

Effect of Supersonic Trim Change on

Airplane Trim Characteristics

In order to determine the effect of the supersonic stabilizer-trim change on the trim characteristics of the full-scale airplane, an analysis of the airplane trim characteristics has been made. In making this analysis, it was assumed that the stabilizer-trim change on the airplane would be identical to the trim change noted on the tail-alone model and that the trim change is the result of flow changes at the tail which are not affected by changes in stabilizer deflection and angle of attack. All of the necessary airplane stability derivatives were estimated and an airplane combat gross weight of 26,260 pounds with center of gravity at 0.25 mean aerodynamic chord was assumed. The calculations were made for level flight at 30,000 feet altitude.

Figure 13 shows the variation with Mach number of trim angle of attack α, trim stabilizer deflection δ, and trim servoplane deflection δ_c. Also shown is a comparison of the trim stabilizer deflection and servoplane deflection required with and without considering the flow change at the stabilizer. The effect of the flow change on angle of attack is insignificant and it is noted that the magnitude of the effect on the stabilizer deflection is less than the magnitude of the flow change. This is a result of the fact that as the flow change occurs the linked flap deflection and resultant servoplane deflection are in such a

direction as to increase the tail-moment contribution in the desired direction. Consequently, the required effective angle of attack of the stabilizer is reduced. It should be pointed out that the magnitude of the servoplane deflection required to overcome the effects of the flow change represents a small percentage of the total servoplane deflection range and that the change is in a stable direction. It is also noted in these figures that between Mach number 0.8 and 1.0 the direction of movement of the servoplane required to maintain trim is unstable in that the stick must be moved back rather than forward as speed is increased. This characteristic is of course not affected by the tail flow change, but is due to the rearward movement of the center of pressure of the airplane and the resultant increase in static stability.

CONCLUDING REMARKS

While the data obtained from this flight test are not entirely con-clusive, the test has served its primary purpose in demonstrating the fact that servoplane effectiveness is maintained at least up to Mach number 1.15 and that there are no serious deficiencies in the behavior of the free-floating stabilizer. The loss of damping near Mach num-ber 1.0 can probably be compensated for by addition of some type of mechanical damper to the stabilizer system. Flight tests to be made with additional models will add materially to the available data on static stability nonlinearities since the servoplane will be pulsed over different but overlapping ranges. In addition, the maximum speed of the tests will be increased and will extend the available data to higher Mach numbers. The flow change at the tail in the supersonic range does not seem to have any serious effect on full-scale airplane performance

so long as the magnitude of the effect of the flow change does not exceed
the available stabilizer deflection range.

Langley Aeronautical Laboratory
        National Advisory Committee for Aeronautics
                Langley Field, Va.

                                        William N. Gardner
                                        Aeronautical Research Scientist

                                        James L. Edmondson
                                        Aeronautical Research Scientist

Approved:

                        Robert R. Gilruth
        Chief of Pilotless Aircraft Research Division

fgs

Figure 1.- Photograph of model-booster combination on launching platform
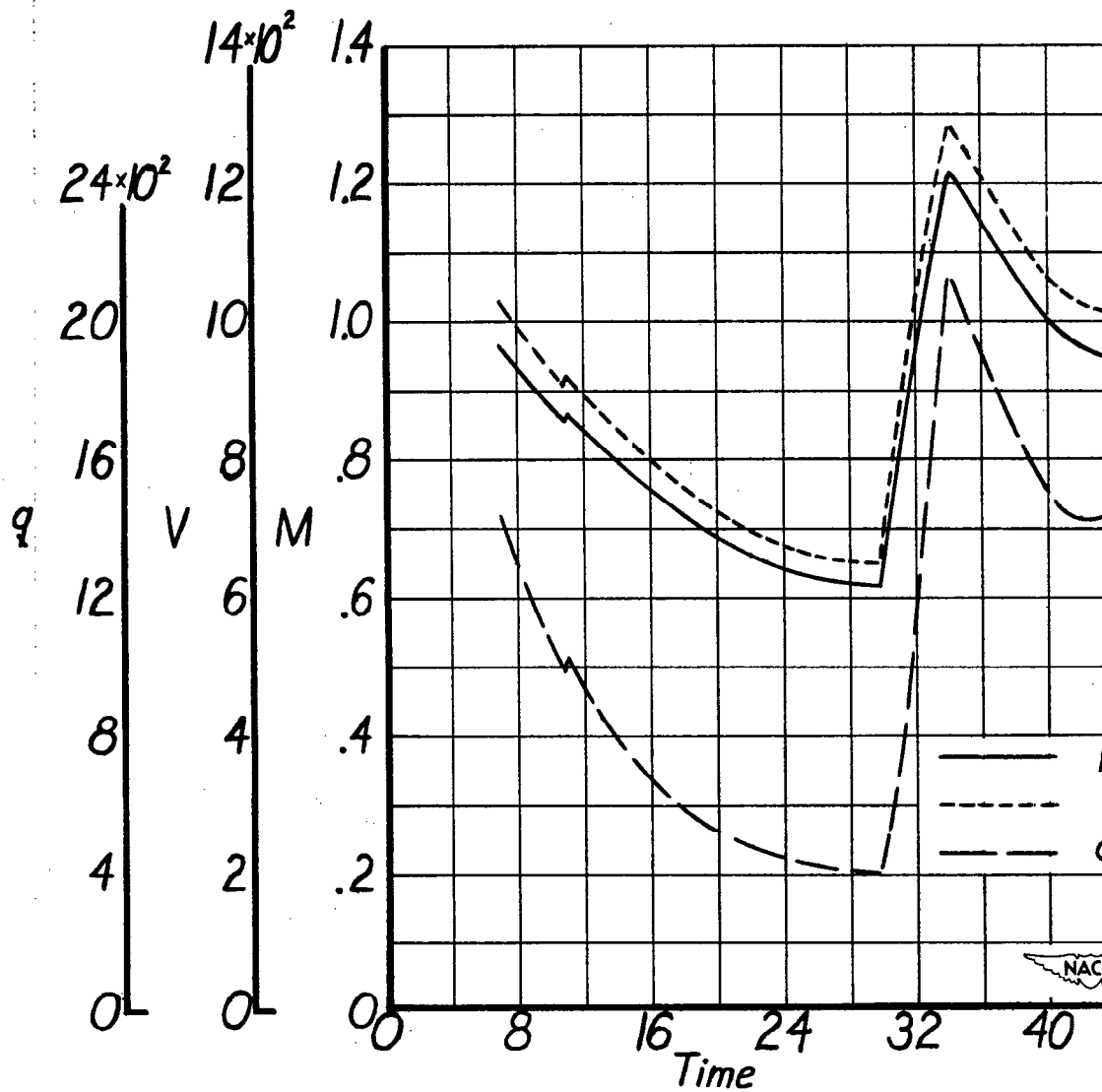
Figure 2.- Time history of Mach number, velocity, and dynamic pressu
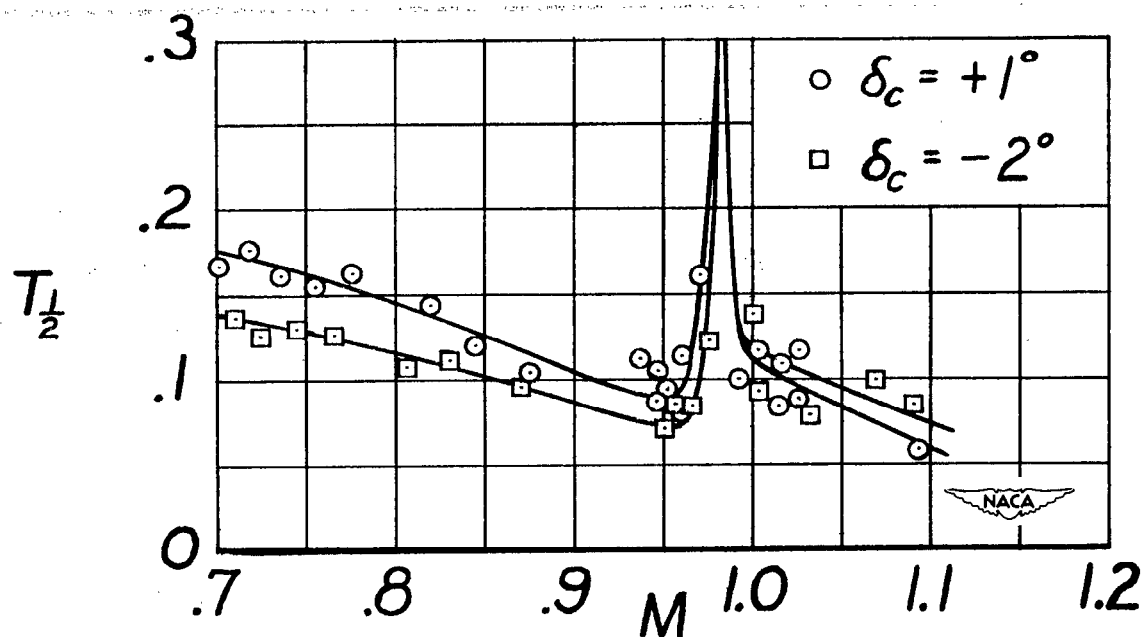
Figure 3.- Variation of time to damp to half-amplitude with Mach number.
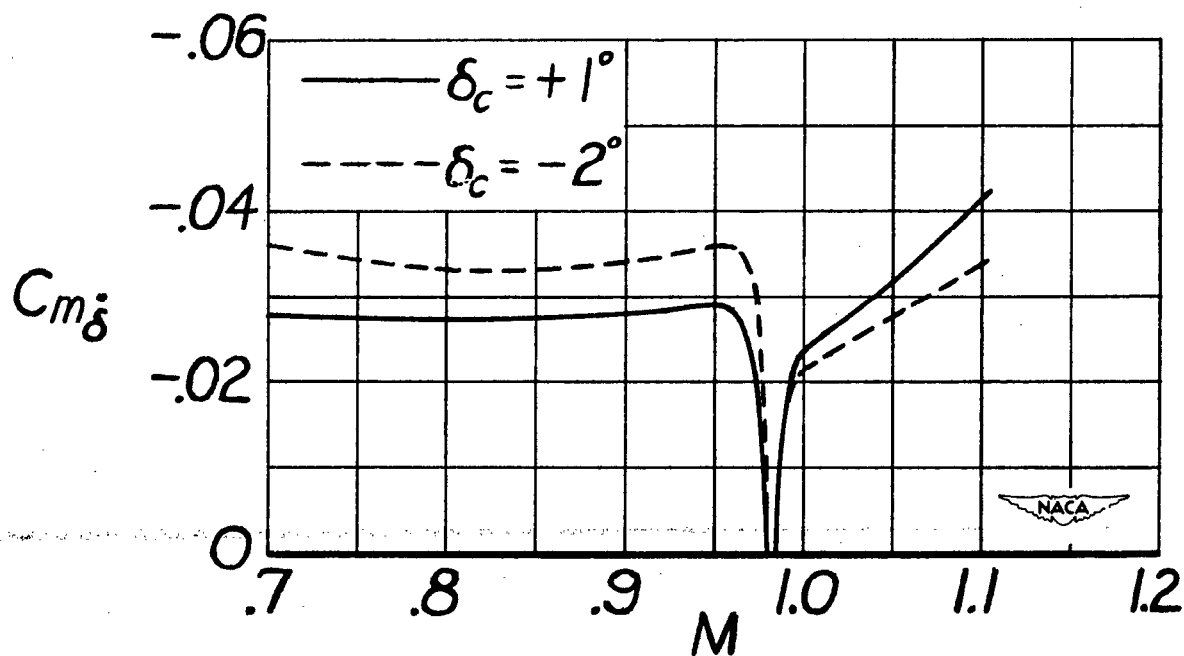
Figure 4.- Variation of tail-damping derivative with Mach number.
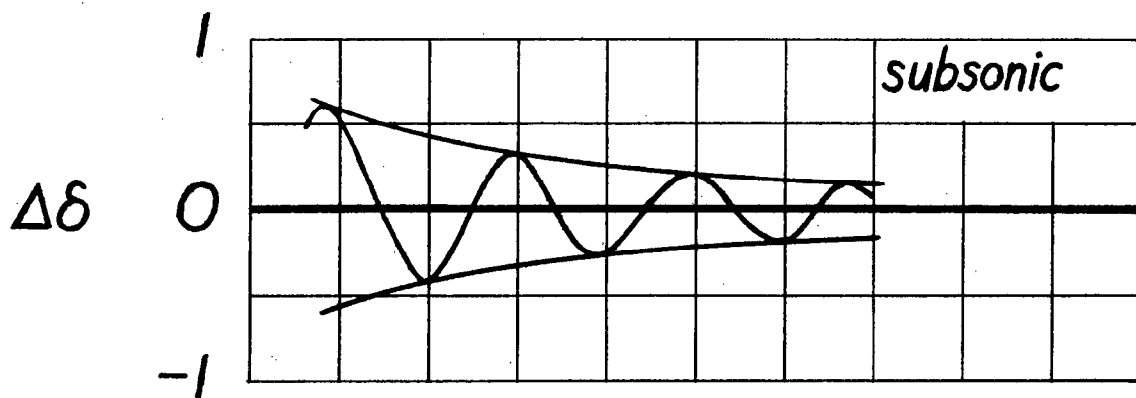
(a) M < 0.9.
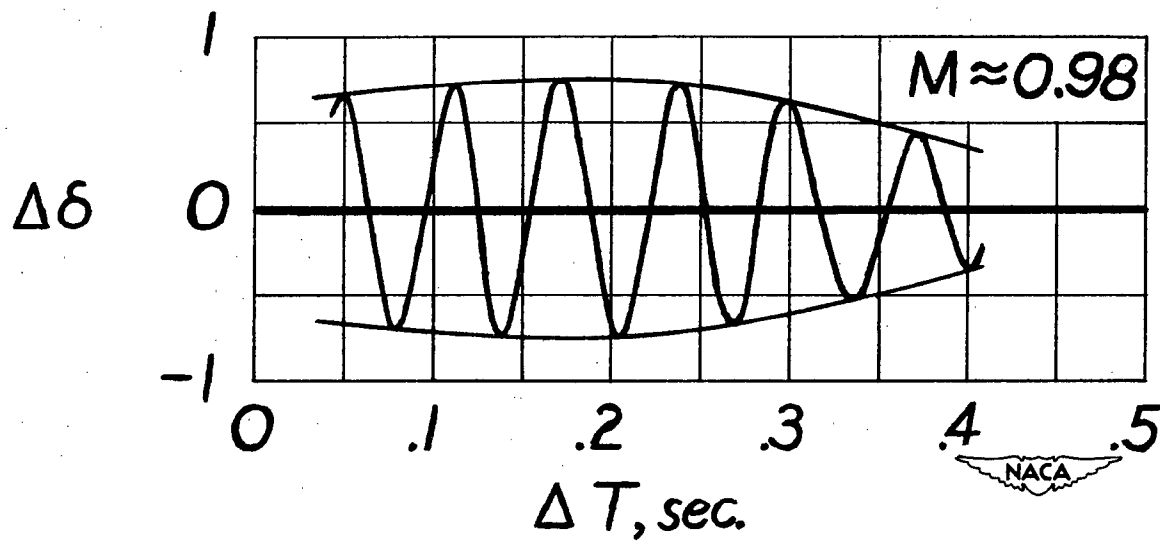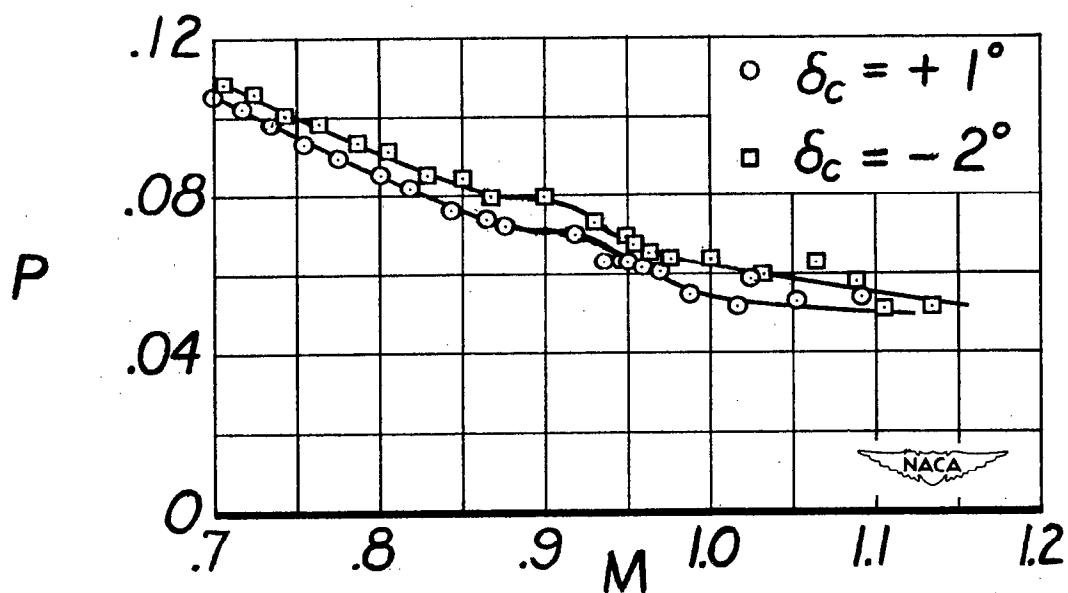
(b) M ≈ 0.98.

Figure 5.- Typical tail-damping envelopes.
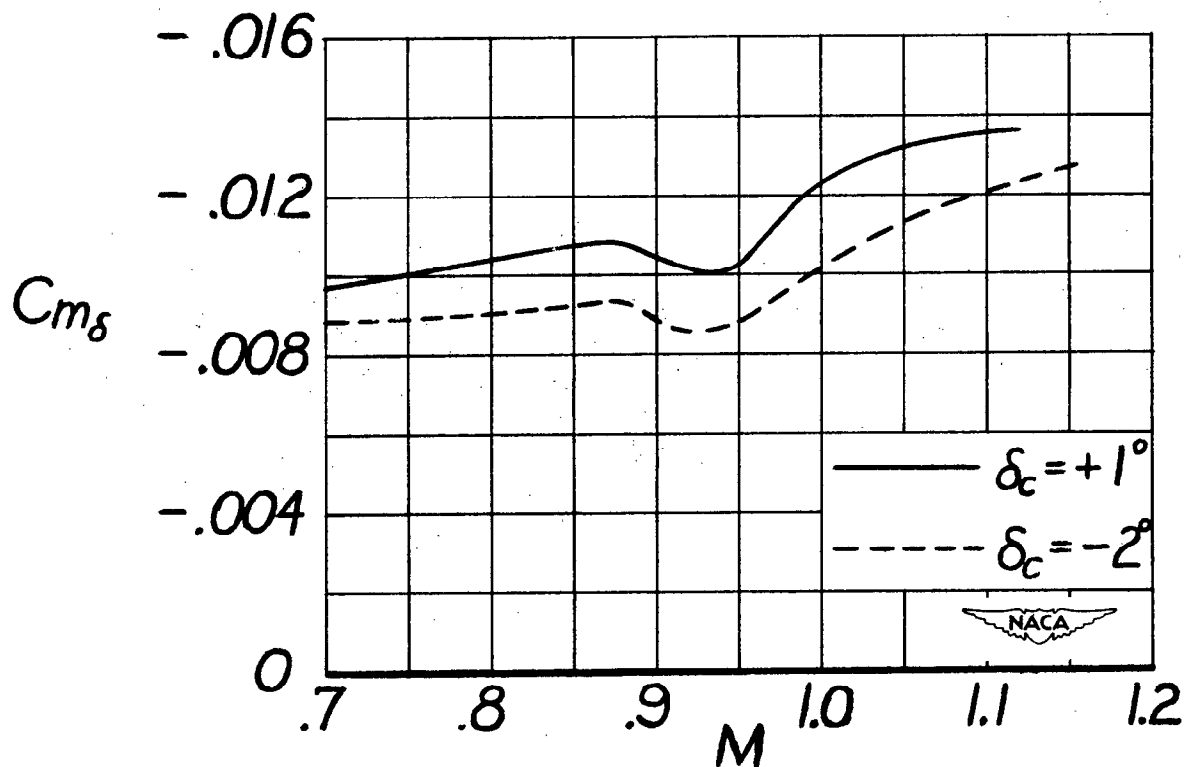
Figure 6.- Variation of period with Mach number.

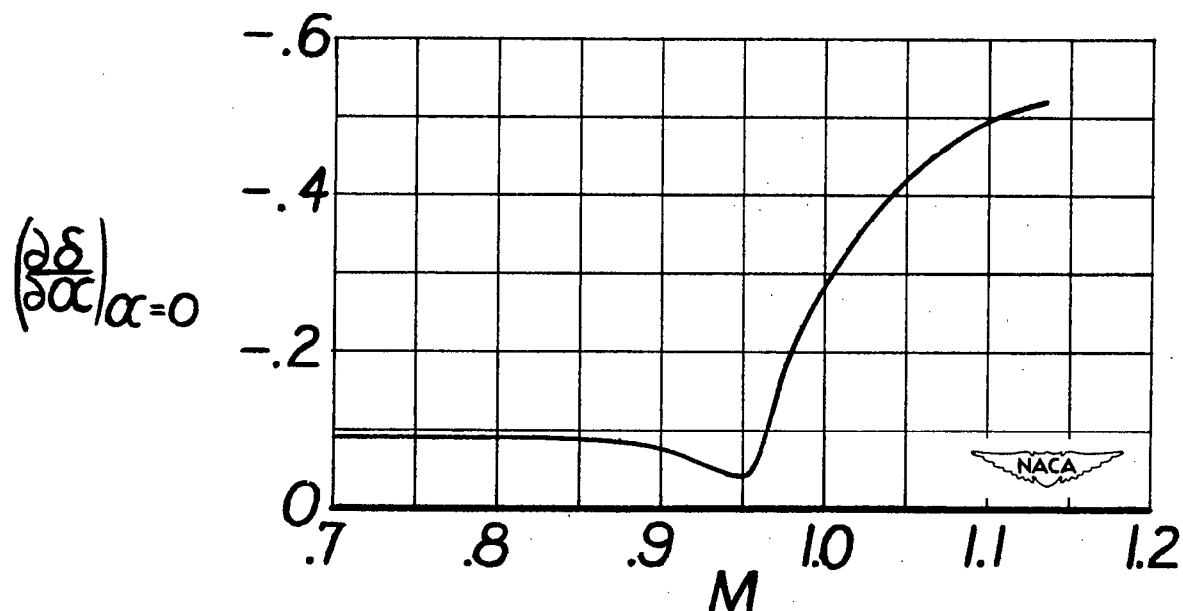Figure 7.- Variation of C_{m_δ} of tail with Mach number.

$$\left(\frac{\partial \delta}{\partial \alpha}\right)_{\alpha=0}$$

Figure 8.- Rate of change of stabilizer deflection with angle of attack
at zero angle of attack, plotted against Mach number.

$$\frac{\partial \delta}{\partial \alpha}$$

M < 0.9
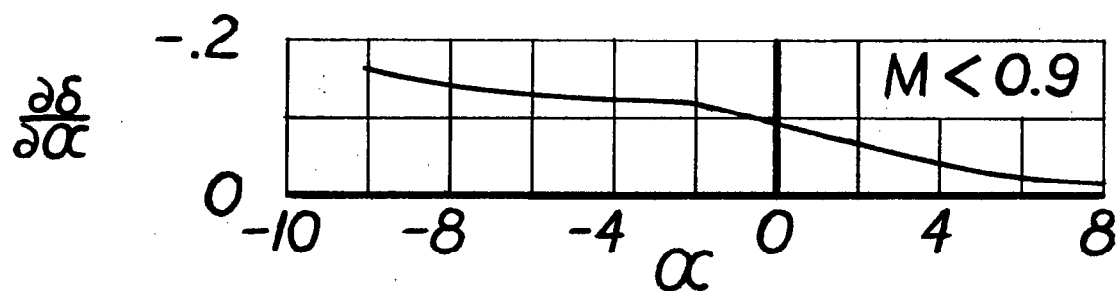
Figure 9.- Rate of change of stabilizer deflection with angle of attack,
plotted against angle of attack.

$$\left(\frac{\Delta\delta}{\Delta\delta_c}\right)_{\alpha=0}$$
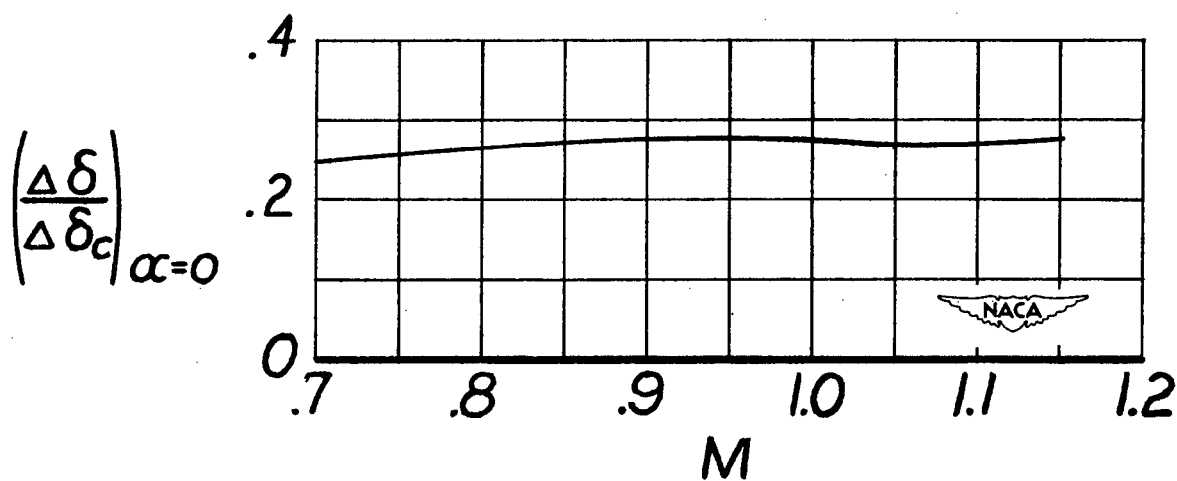
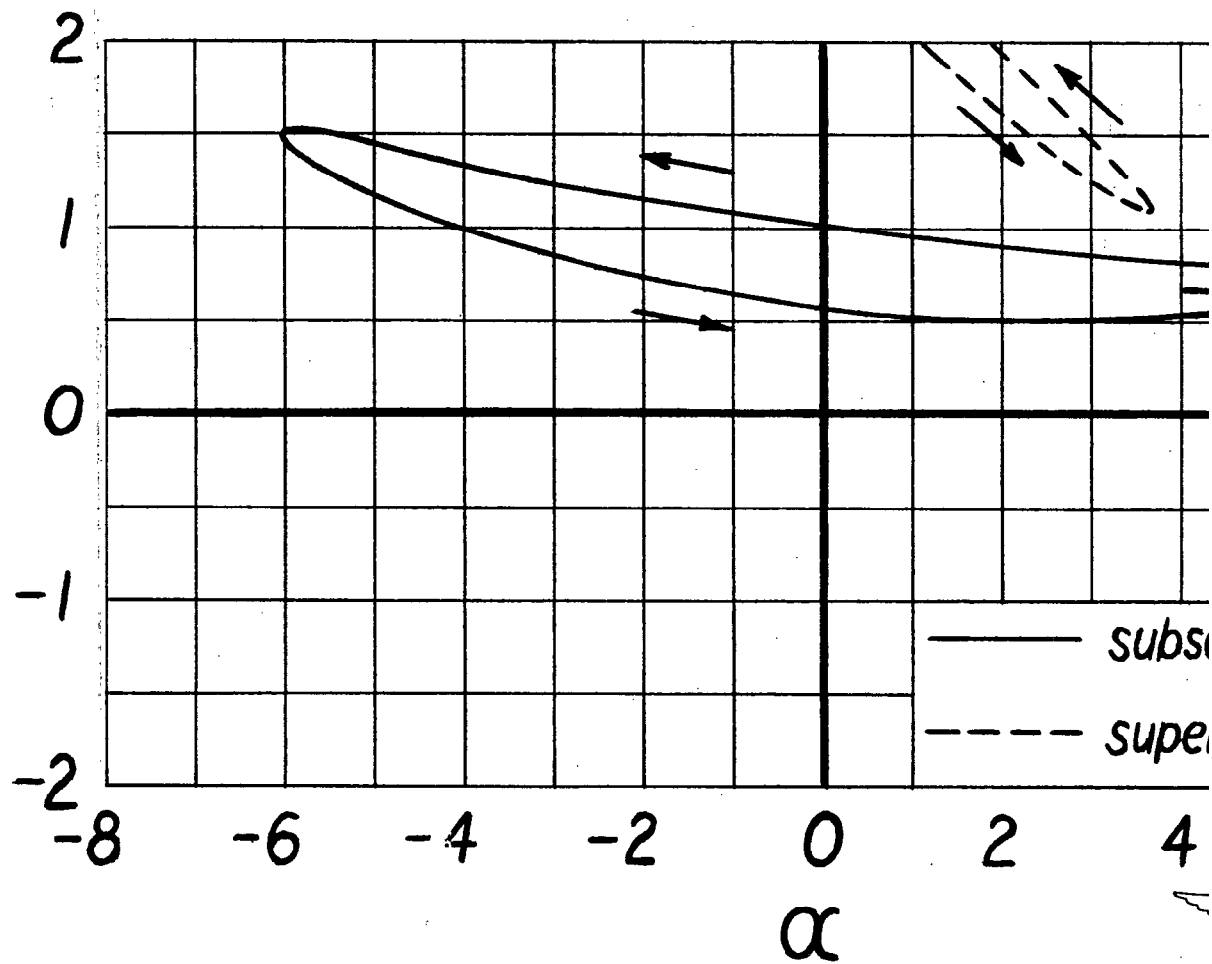Figure 10.- Variation of servoplane effectiveness with Mach number.

Figure 11.- Variation of trim stabilizer deflection with angle of a⁻
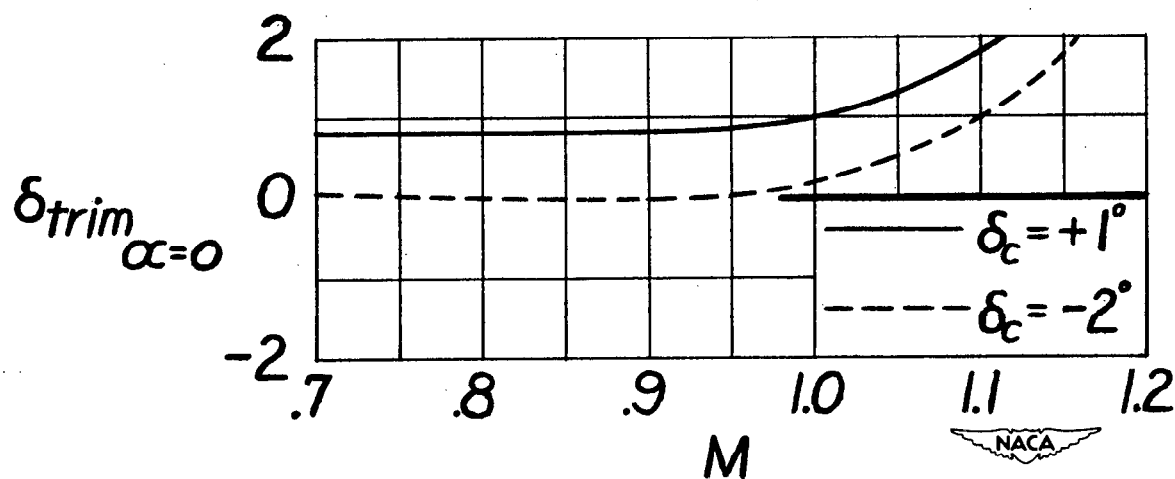
Figure 12.- Variation of trim stabilizer deflection at zero angle of attack with Mach number.
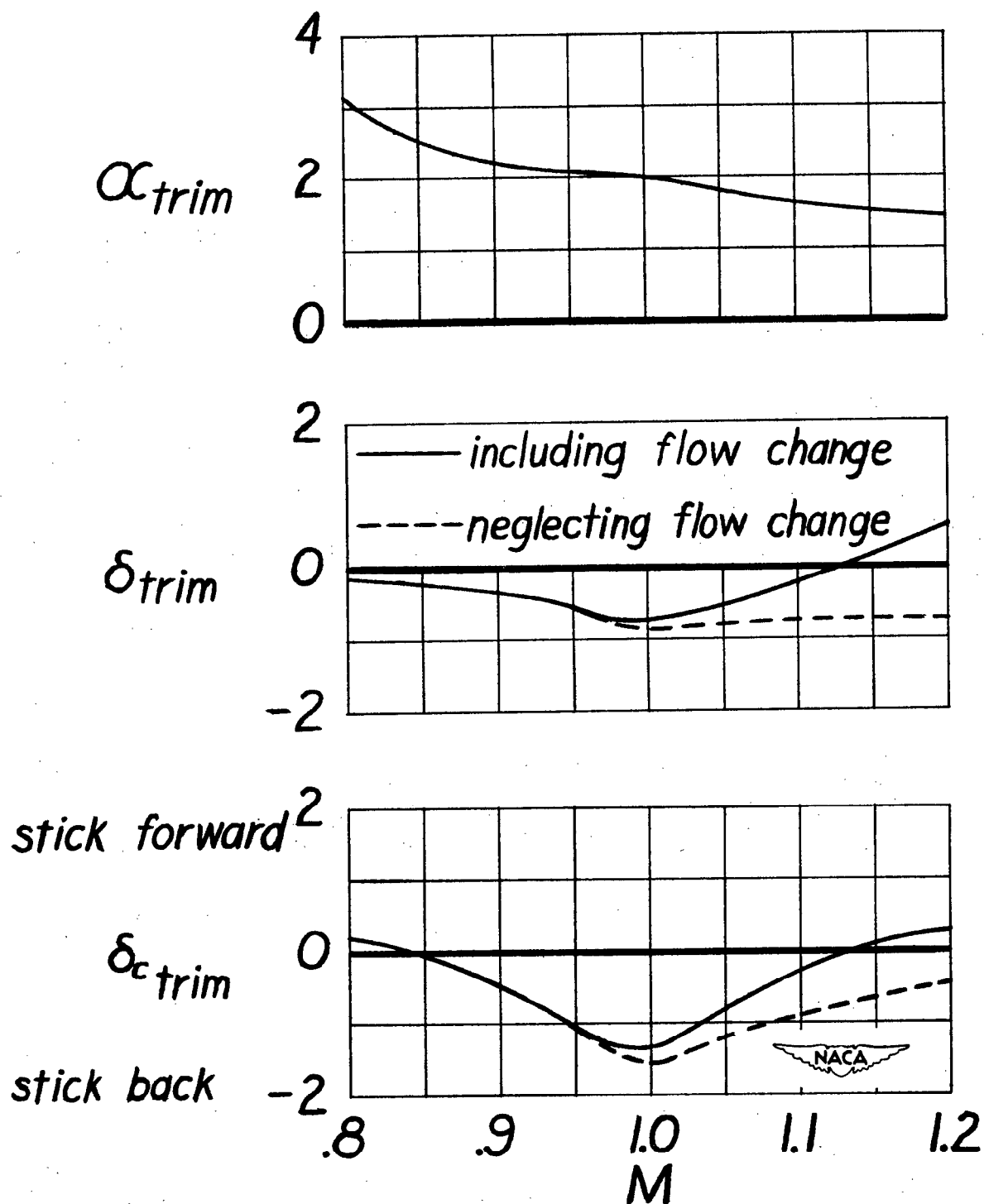
Figure 13.- Variation of airplane trim with Mach number.